Journal of Catalysis **185,** 445–453 (1999)
Article ID jcat.1999.2477, available online at http://www.idealibrary.com on IDEAL®

Synthesis of Butyl-α and β-D-Glucopyranosides in the Presence of Dealuminated H–Y Faujasites: Kinetic Study, Mechanism, Stereoelectronic Effects, and Microreversibility Principle

Jean-François Chapat, Annie Finiels, Jacques Joffre, and Claude Moreau[1]

Laboratoire de Matériaux Catalytiques et Catalyse en Chimie Organique, UMR CNRS-ENSCM 5618, Ecole Nationale Supérieure de Chimie, 8, Rue de l'Ecole Normale, 34296 Montpellier Cedex 5, France

Received December 21, 1998; revised February 23, 1999; accepted February 23, 1999

The glycosylation reaction between D-glucose and *n*-butanol has been investigated over various dealuminated HY zeolites with Si/Al ratios from 2.5 to 100. In this way, butyl-α- and β-D-glucofuranosides and -pyranosides are readily synthesized at temperatures from 363 to 383 K and with a butanol/glucose ratio from 5 to 40. From the systematic study of the glycosylation reaction, a kinetic scheme involving both consecutive and competitive steps has been proposed. Butyl-D-glucofuranosides and butyl-D-glucopyranosides are primary products, butyl-D-glucofuranosides being then quantitatively converted into their pyranoside form. The use of microporous catalysts, associated with their shape selectivity properties, reduces the amount of oligomers and increases the amount of β-D-glucopyranosides in a significant manner. The β/α anomeric ratios observed are then discussed in terms of stereoelectronic effects which are, according to the principle of microreversibility, of the same nature as those reported for the reverse reaction, i.e., hydrolysis of alkyl-D-glucopyranosides.

Key Words: **glycosylation; alkylglucosides; surfactants; zeolites; stereoelectronic effects.**

INTRODUCTION

Alkylglycosides are a new class of nonionic surfactants which find applications in cosmetics, food emulsifient, and detergency (1, 2) because of their nontoxic and biodegradable properties (3). As due to their composition, i.e., a glucose hydrophilic moiety associated with a long hydrophobic alkyl chain of a fatty alcohol, alkylglycosides present lyotropic and thermotropic properties as liquid crystals (4). Although the first synthesis of alkylglycosides was described a hundred years ago by Fischer (5), this reaction is always under investigation (6–8). Generally, protection and deprotection steps are required in order to obtain alkylglycosides with a high selectivity. However, some authors have already shown that alkylglycosides could be synthesized directly using heterogeneous catalysts as, for example, macroporous sulfonated resins (9, 10) and acid clays (11). Recently, it was shown that the use of acid zeolites (12) could avoid the principal drawback of the direct Fischer synthesis, i.e., the formation of oligomer species.

We report in the present paper the synthesis of butyl-D-glucosides over dealuminated HY faujasites by acetalization of D-glucose with *n*-butanol. A kinetic study of this reaction has been carried out in order to clarify the mechanism. On the other hand, it was interesting to control the stereoselectivity of the reaction since the tensioactive properties of α and β anomers are quite different (13, 14). The influence of textural properties of various zeolites such as HY or HBEA on the anomeric β/α ratio of furanosides and pyranosides is then discussed in terms of shape selective properties of zeolites and in terms of stereoelectronic effects.

EXPERIMENTAL

Materials

Anhydrous α-D-glucose, *n*-butanol, and *p*-toluene sulfonic acid (PTSA) were supplied by Aldrich and used without further purification. Butyl-D-glycosides were purified by preparative chromatography on Chromagel 60A with ethyl acetate/methanol 98/2 (v/v) as the eluent. They were identified by ^{13}C NMR spectroscopy and by comparison with the data from the literature (9).

Catalysts

Dealuminated H-form zeolites were obtained from Degussa, PQ Zeolites, and Uetikon. The different data concerning the catalysts used, origin, and Si/Al ratios as well as their acidity measured by thermodesorption of ammonia are reported in Table 1.

[1] To whom correspondence should be addressed. Fax: +33-(0)467 144 349; E-mail: cmoreau@cit.enscm.fr.

0021-9517/99 $30.00

TABLE 1

Zeolites Used for Glycosylation of D-Glucose with *n*-Butanol

Zeolite	Si/Al	Acidity (meq $H^+ g^{-1}$)
HY (UETIKON)	2.5	0.94
HY (PQ-CBV 712)	5.7	0.82
HY (PQ-CBV 720)	15	0.56
HY (PQ-CBV 740)	21	0.30
HY (PQ-CBV 760)	25.5	0.22
HY (PQ)	29	0.16
HY (PQ)	40	0.15
HY (DEGUSSA)	100	0.06
HBEA (PQ-CP811)	12.5	0.92

Work-up Procedure

As described in a preliminary work, the procedure was typically as follows: 50 ml of *n*-butanol (0.54 mol), 4.80 g of α-D-glucose (0.027 mol), and 3 g of freshly calcined zeolite (773 K for 6 h) were poured into a magnetically stirred (1000 rpm) 100 ml glass reactor operating in a batch mode. Zero time was taken to be when the temperature reached 383 K. The reaction was thus performed with an optimal butanol/glucose molar ratio of 20 in the presence of 6 wt% of catalyst. D-glucose was completely dissolved in butanol during the formation of butyl-D-glucosides so that there is no kinetic limitation due to glucose solubilization.

Analyses

Samples were withdrawn periodically from the reactor, filtered, and analyzed by HPLC. Analyses were performed using a Shimadzu LC-6A pump and a refractive index RID-6A detector. The column used was a BIORAD HPX-87C (300×7.8 mm) thermostated at 353 K. Deionized water was the eluent (0.5 ml/min), and D-sorbitol was the external standard.

Kinetic Modeling

The initial rate constants were deduced from the experimental plots of concentrations in all species formed vs reaction time by curve fitting and simulation using the AnaCin software (16). This kinetic treatment implies all reaction steps to be first order in reactants.

RESULTS AND DISCUSSION

Kinetic Studies

(a) Mass transfer. In order to establish the kinetic rate law, the chemical regime conditions must be first determined. For the study of the external diffusion of the reactants to the catalyst surface (17), the agitation speed and the weight of the catalyst were varied.

The initial reaction rate for the disappearance of glucose is independent of the agitation speed above 400 rpm. A 1000 rpm agitation speed was therefore used in all further experiments. The initial reaction rate increases proportionally with catalyst weight up to a maximum for 3 g catalyst weight. Further experiments were then achieved in the presence of 3 g of zeolite (6% of the total weight).

(b) Pore diffusion. The importance of internal diffusion can be estimated from the criterion of Weisz (18) $\Phi = dN/dt \times 1/C_0 \times R^2/D_{\text{eff}}$, in which dN/dt is the reaction rate (mol cm^{-3} s^{-1}), C_0 is the initial reactant concentration (mol cm^{-3}), R is the particle radius (cm), and D_{eff} is the effective diffusivity coefficient (cm^2 s^{-1}). The intracrystalline diffusion limitation can be ruled out when $\Phi < 0.1$. Under our conditions, $dN/dt = 3.08 \times 10^{-7}$ mol cm^{-3} s^{-1}, $C_0 = 0.533 \times 10^{-3}$ mol cm^{-3}, and $R = 0.25 \times 10^{-4}$ cm. This requires $D_{\text{eff}} > 10^{-12}$ cm^2 s^{-1}, a reasonable value for the diffusivity coefficient of that type of molecule in microporous systems.

(c) Energies of activation. The influence of the temperature on the reaction rates was investigated in the range 363–383 K. The energies of activation calculated by the Arrhenius law are reported in Table 2. These values are on the same order of magnitude ($\sim$30 kcal mol^{-1}) and show that the reaction is not governed by external diffusion limitations (17). Moreover, it can be noticed that the energies of activation are slightly lower for furanosides than for pyranosides, thus confirming that, as in homogeneous catalysis, furanosides are the kinetic products and pyranosides the thermodynamic ones.

(d) Reaction scheme. Under the experimental conditions used (4.80 g of D-glucose, 50 ml of *n*-butanol, 3 g of freshly calcined zeolite, 383 K, and 1000 rpm of agitation speed), it has been shown that the reaction could be taken as obeying chemical regime conditions. A typical concentration vs time profile for the glycosylation of butanol at 383 K is presented in Fig. 1. This figure shows the disappearance of D-glucose and appearance of the various identified products (butyl-α and β-D-glucofuranosides and butyl-α and β-D-glucopyranosides) as a function of time.

TABLE 2

Initial Reaction Rates ($\times 10^5$ mol s^{-1}) for the Disappearance of D-Glucose and the Appearance of Butyl-D-Glucosides at Different Temperatures and Corresponding Energies of Activation

T (K)	D-glucose	Butyl-β-D-furanoside	Butyl-α-D-furanoside	Butyl-β-D-pyranoside	Butyl-α-D-pyranoside
363	0.130	0.075	0.050	0.010	0.005
373	0.440	0.235	0.145	0.030	0.015
383	1.540	0.675	0.585	0.130	0.075
Ea (kcal mol^{-1})	35	31	35	36	38

Note. 4.8 g of D-glucose, 50 ml of *n*-butanol, 6 wt% of freshly calcined HY15, 1000 rpm.

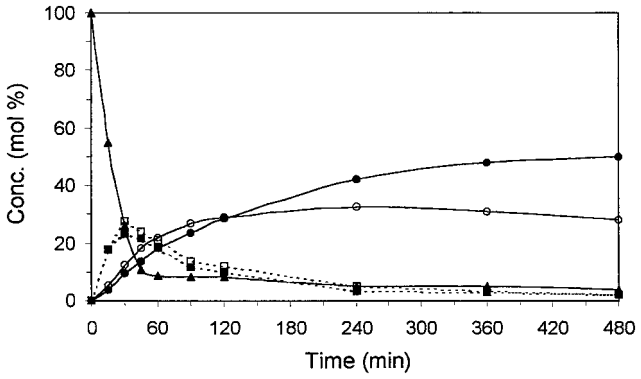

FIG. 1. Run profile for glycosylation of D-glucose (4.8 g) with *n*-butanol (50 ml) in the presence of freshly calcined HY15 (6 wt%) at 383 K and 1000 rpm of agitation speed (▲, α-D-glucose; ●, butyl-α-D-glucopyranoside; ❍, butyl-β-D-glucopyranoside; ■, butyl-α-D-glucofuranoside; □, butyl-β-D-glucofuranoside).

From Fig. 1, it is shown that butyl-D-glucofuranosides are the major primary products of the reaction (kinetic products). Their concentration passes through a maximum and then decreases with time to give the thermodynamically more stable butyl-D-glucopyranosides (19, 20). However, it is worth noting that butyl-D-glucopyranosides are also primary products. According to these observations, and to previously published works (21, 22), a general reaction scheme can be advanced for the glycosylation reaction, involving both parallel and successive reactions (Scheme 1).

(e) Kinetic results. Such a reaction scheme has been confirmed by the use of the kinetic AnaCin modeling software by providing the best fit between calculated curves and experimental data (Fig. 2). The mass balance is assumed to be oligoglucosides without further distinction. The pseudo first-order rate constants resulting from AnaCin curves are reported in Table 3. From the rate constant values, it is then possible to calculate the initial disappearance rate of D-glucose, $r_0 = kC_0$. On the other hand, initial reaction rates can also be calculated as the tangents, at zero time, to the experimental concentration vs time curves. A fairly good

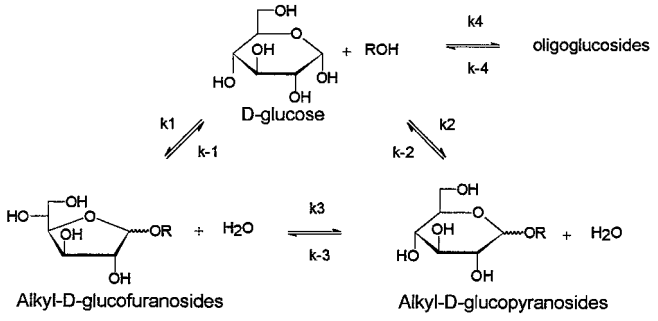

SCHEME 1. Simplified reaction scheme for glycosylation of D-glucose with *n*-butanol.

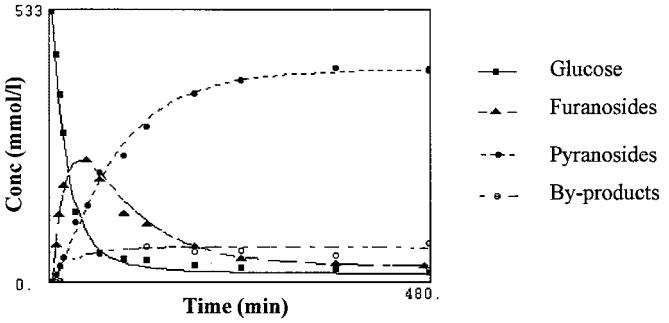

FIG. 2. AnaCin modeling plot for glycosylation of D-glucose (4.8 g) with *n*-butanol (50 ml) in the presence of freshly calcined HY15 (6 wt%) at 383 K and 1000 rpm of agitation speed.

agreement is obtained between the two modes of calculation of the initial reaction rates (Table 4).

(f) Influence of the initial concentration of D-glucose. We have measured initial rates at different initial concentrations in D-glucose while the concentration of butanol is kept constant. Figure 3 shows the initial reaction rate evolution with the initial concentration of D-glucose. As it can be seen from Fig. 3, the initial rate increases, reaches a maximum when the D-glucose concentration is about 0.3–0.5 M, and then decreases. This maximum may indicate a Langmuir–Hinshelwood type mechanism with both reactants adsorbed (15).

(g) Kinetic law. As already proposed in the case of hydroxymethylation of furfuryl alcohol in the presence of zeolites (23), adsorption of reactants could take place on two types of catalytic sites. Indeed, in the hypothesis of adsorption on Brønsted sites for both alcohol and glucose, two species positively charged could not react together in an acetalization reaction. Consequently, we assume that the molecules of glucose and butanol are adsorbed on adjacent but different places: glucose on the protonic sites and butanol on the framework by hydrophobic interactions between hydrocarbon chain of alcohol and silicon atoms. An enhancement of the nucleophilicity of the hydroxyl group of the alcohol could not be ruled out by interaction between the hydrogen of the hydroxyl group and an oxygen atom of the framework. With such an assumption, the rate for the

TABLE 3

Calculated Pseudo First-Order Rate Constants (min^{-1}) from AnaCin Kinetic Software

*k*1	*k*-1	*k*2	*k*-2	*k*3	*k*-3	*k*4	*k*-4
0.036	0.005	0.004	0.001	0.013	0	0.005	0.001

Note. 4.8 g of D-glucose, 50 ml of *n*-butanol, 6 wt% of freshly calcined HY15, 383 K, 1000 rpm.

TABLE 4

Influence of the Si/Al Ratio on the Initial Rate of Disappearance of D-Glucose

Zeolite (Si/Al ratio)	r_0 AnaCin ($\times 10^5$ mol s^{-1})[a]	r_0 Graphic ($\times 10^5$ mol s^{-1})[b]
HY (2.5)	0.020	0.020
HY (5.7)	1.290	1.080
HY (15)	1.780	1.540
HY (21)	0.730	0.690
HY (25.5)	0.560	0.525
HY (29)	0.530	0.420
HY (40)	0.300	0.270
HY (100)	0.130	0.110

[a] Calculation from AnaCin software.
[b] Calculation from the slope of the tangent at the origin.

reaction can be written as

$$r = k\frac{\lambda_G[G]}{(1+\lambda_G[G])}\frac{\lambda_A[A]}{(1+\lambda_A[A])},$$

where $[G]$ and $[A]$ are the concentrations of glucose and of butanol and λ_G and λ_A their respective adsorption constants. Taking into account that butanol is in large excess with respect to glucose, the following simplified equation is obtained,

$$r = \frac{-d[G]}{dt} = k\frac{\lambda_G[G]}{(1+\lambda_G[G])},$$

which finally leads, after integration, to the kinetic rate equation below:

$$\frac{1}{\lambda_G}\ln\frac{[G]_0}{[G]} + ([G]_0 - [G]) = kt.$$

As shown in Fig. 3, the initial reaction rate is maximum and approximatively constant (1.5×10^{-5} mol s^{-1}) for initial glucose concentrations between 0.3 and 0.5 M, with a reaction relative order close to zero, $r_0 = k = 1.5 \times 10^{-5}$ mol s^{-1}.

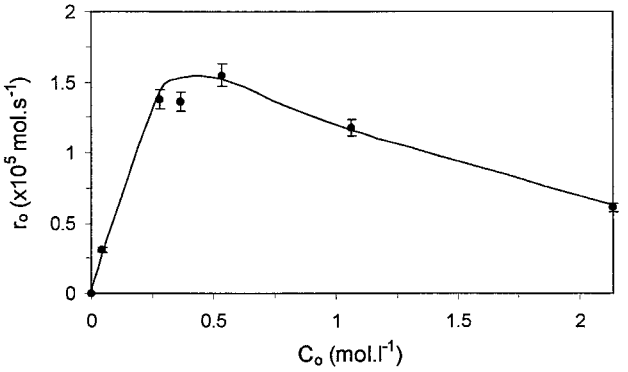

FIG. 3. Plot of initial rate of disappearance of D-glucose versus initial concentration in D-glucose (10% error bars) for glycosylation of D-glucose (4.8 g) with *n*-butanol (50 ml) in the presence of freshly calcined HY15 (6 wt%) at 383 K and 1000 rpm of agitation speed.

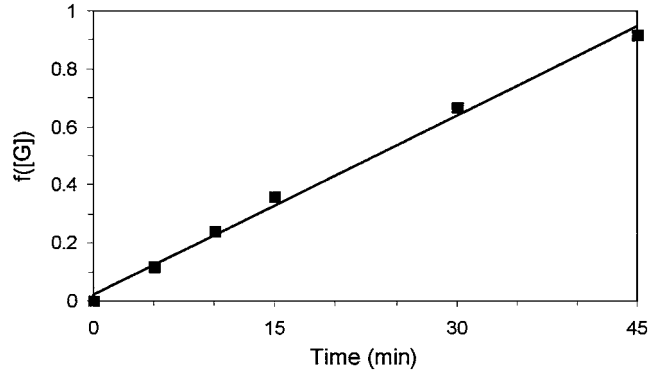

FIG. 4. Plot of $f([G])$ versus reaction time (min) for glycosylation of D-glucose (4.8 g) with *n*-butanol (50 ml) in the presence of freshly calcined HY15 (6 wt%) at 383 K and 1000 rpm of agitation speed.

At low initial D-glucose concentrations, the rate equation is reduced to $k\lambda_G[G]_0$. A λ_G value can thus be calculated, equal to 5, from known values of $[G]_0$ (0.044 mol l^{-1}), r_0 (0.31×10^{-5} mol s^{-1}), and k (1.5×10^{-5} mol s^{-1}).

By plotting now $f([G]) = 1/\lambda_G \ln([G]_0/[G]) + ([G]_0 - [G])$ as a function of reaction time (Fig. 4), a straight line is obtained and the rate constant deduced from the slope (1.7×10^{-5} mol s^{-1}) is in good agreement with the value obtained from experimental data (1.5×10^{-5} mol s^{-1}).

(h) Influence of the Si/Al ratio. As previously mentioned, using zeolites in glycosylation decreases the formation of by-products such as oligoglucosides (12). Another interesting feature of using zeolites is the possibility to control their acidity by dealumination. The acid strength of a given site increases when the number of Al atoms in the next nearest neighbor positions (NNN) decreases. A completely isolated aluminum tetrahedron has zero NNN and is consequently the strongest type of framework Brønsted site. This is the case for Faujasite-type zeolites with Si/Al ratios higher than 6.8 (24). As shown in the kinetic part, the glycosylation reaction requires Brønsted acid sites for adsorption of glucose through protonation of the anomeric oxygen. Acetalization then occurs by a nucleophilic attack of butanol.

Glycosylation of butanol was therefore studied over a series of dealuminated HY zeolites with different framework Si/Al ratios (from 2.5 to 100). The initial reaction rates for the disappearance of glucose are reported in Table 4. By plotting those reaction rates as a function of the Si/Al ratio (Fig. 5), it can be seen that the activity increases up to a Si/Al ratio equal to 15 and then decreases significantly. As already reported for other reactions, this Si/Al ratio of 15 is representative of the balance between the number and the strength of the acid sites for HY zeolites (25).

In Fig. 6, the turn-over frequencies (TOF), calculated by dividing the initial reaction rate by the number of acid

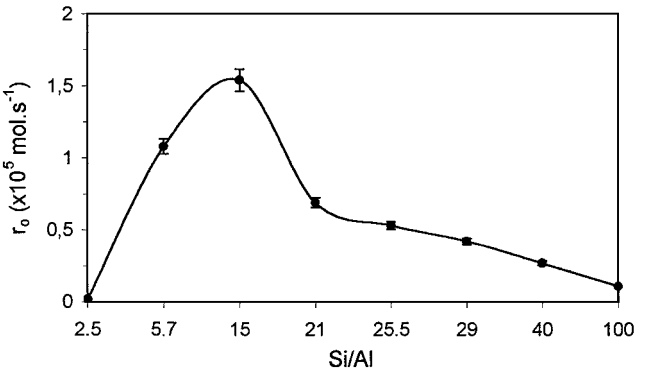

FIG. 5. Plot of initial rate of disappearance of D-glucose versus Si/Al ratio (10% error bars) for glycosylation of D-glucose (4.8 g) with *n*-butanol (50 ml) in the presence of freshly calcined HY (6 wt%) at 383 K and 1000 rpm of agitation speed.

sites as determined by TPD of ammonia (Table 1), are now expressed as a function of the Si/Al ratio. It can be seen that the activity per site is maximum and nearly constant from Si/Al = 15 to 29. For higher Si/Al ratios, the catalyst is too hydrophobic for a good adsorption of D-glucose and the TOF slightly decreases. On the contrary, for HY 2.5, glucose is preferentially adsorbed and the reaction may then be limited by both diffusion and adsorption of *n*-butanol. As recently reported by Corma *et al.* (26), "a highly hydrophilic reactant (glucose) and a much more hydrophobic one (*n*-butanol) have to diffuse through the pores and adsorb in the zeolite." Consequently, zeolites having too low or too high Si/Al ratios are not efficient catalysts for the reaction considered.

Selectivity of Zeolites

(a) Comparison of different catalysts. The behavior of the HY zeolite with a Si/Al ratio of 15 was compared with that of a HBEA zeolite with a Si/Al ratio of 12.5, known to be an efficient catalyst for glycosylation (12). Para-toluene sulfonic acid (PTSA) was used as the reference to homogeneous catalysis. The experimental results obtained are shown in Table 5. Except the amount of *p*-toluene sulfonic acid (0.05 g), all other parameters are unchanged (4.80 g of D-glucose, 50 ml of *n*-butanol, 6 wt% zeolite, 383 K, 1000 rpm). Figures 7 and 8 illustrate glucose conversion vs time plots for HBEA and PTSA catalysts, respectively. The most striking feature between those two catalysts is the important difference observed for the β/α ratio of pyranosides in the first two hours of reaction. Concerning the formation of butyl α- and β-D-glucofuranosides, the stereoselectivity of the reaction is not controlled because the α,β anomerization is too fast and the thermodynamic ratio is rapidly obtained (27, 28), so that the most stable β-furanoside is always preferentially formed with a β/α ratio around 1.2. Concerning the formation of butyl α- and β-D-glucopyranosides, plots of β/α ratio of pyranosides vs glucose conversion for HY15, HBEA12.5, and PTSA catalysts are reported in Fig. 9. The β/α ratio of pyranosides is around 1.5 for HY15 and around 0.7 for HBEA12.5, whereas PTSA shows an intermediate β/α ratio around 1. At nearly a complete conversion of glucose, the thermodynamic ratio β/α of 0.5 is obtained.

TABLE 5

Comparison of the Different Types of Catalysts Used for Glycosylation

Catalyst	r_0 glucose ($\times 10^5$ mol s^{-1})	Mass balance (%)
HY 15	1.540	91[a]
HBEA 12.5	1.500	75[b]
PTSA	1.460	85

Note. Products adsorbed on the catalyst ([a]5 and [b]10%) were recovered by extraction of the solid with water.

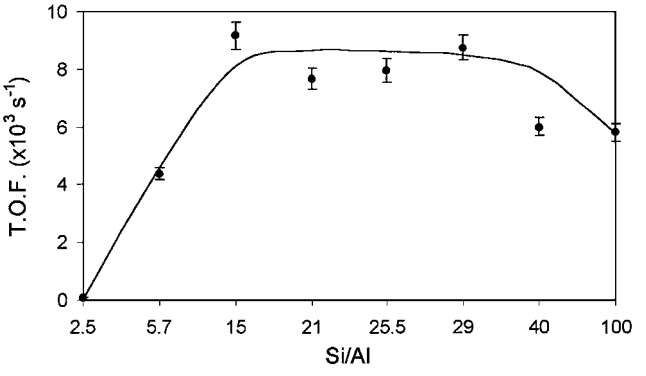

FIG. 6. Turn-over frequency versus framework Si/Al ratio (10% error bars) for glycosylation of D-glucose (4.8 g) with *n*-butanol (50 ml) in the presence of freshly calcined HY (6 wt%) at 383 K and 1000 rpm of agitation speed.

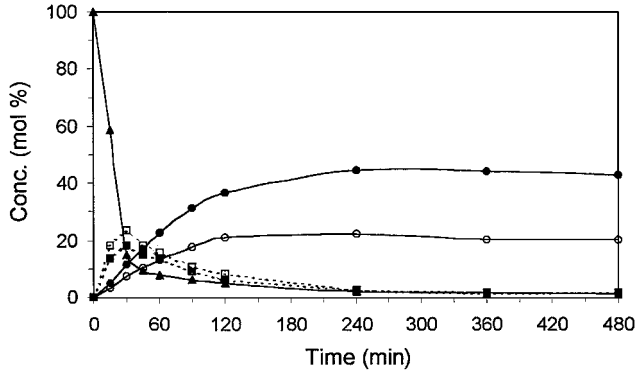

FIG. 7. Run profile for glycosylation of D-glucose (4.8 g) with *n*-butanol (50 ml) in the presence of freshly calcined HBEA12.5 (6 wt%) at 383 K and 1000 rpm of agitation speed (▲, α-D-glucose; ●, butyl-α-D-glucopyranoside; ○, butyl-β-D-glucopyranoside; ■, butyl-α-D-glucofuranoside; □, butyl-β-D-glucofuranoside).

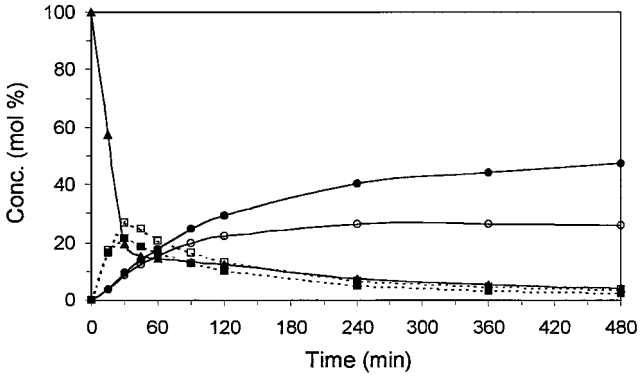

FIG. 8. Run profile for glycosylation of D-glucose (4.8 g) with *n*-butanol (50 ml) in the presence of PTSA (0.05 g) at 383 K and 1000 rpm of agitation speed (▲, α-D-glucose; ●, butyl-α-D-glucopyranoside; ❍, butyl-β-D-glucopyranoside; ■, butyl-α-D-glucofuranoside; □, butyl-β-D-glucofuranoside).

TABLE 6

Energies and Critical Diameters of Reactants and Products

Reactants and products	Energy (kcal mol^{-1})[a]	Critical diameter (Å)[b]
α-D-glucofuranose	11.9	5.4
β-D-glucofuranose	11.5	5.9
α-D-glucopyranose	5.0	6.4
β-D-glucopyranose	5.3	6.4
α-butyl-D-glucofuranoside	13.5	5.1
β-butyl-D-glucofuranoside	13.2	5.7
α-butyl-D-glucopyranoside	6.3	6.3
β-butyl-D-glucopyranoside	6.6	6.3

[a] Hyperchem calculated energies must be considered as relative energies.

[b] Estimated critical diameter after projection of molecules in different plans (±0.3 Å).

In a previous paper (15), we explained that the increase in the selectivity to butyl β-D-glucopyranosides over HY15 zeolite could result from the shape selective properties of that kind of catalyst, thus favoring the formation of the β-anomer with an equatorial OR group over that of the expected more sterically hindered α-anomer with an axial OR group. However, the results obtained with the HBEA zeolite do not agree with that simple explanation since the β selectivity should have increased as due to the more confined crystalline network in HBEA catalyst (tridirectional framework with straight 7.6 × 6.4 Å channels connected by 5.5 Å channels) than in HY15 (tridirectional framework with 7.4 Å windows connecting 11.8 Å spherical cavities) (29). In order to account for this unexpected stereoselectivity order, a molecular modeling simulation was performed to appreciate the size of the molecules involved.

(b) Molecular modeling. Molecular modeling simulations were performed with Hyperchem 4.5, a well-known molecular modeling software, using the molecular mechanics force field AmberS. This force field was designed for modeling oligosaccharides (30) presenting glycosidic linkages as alkylglucosides.

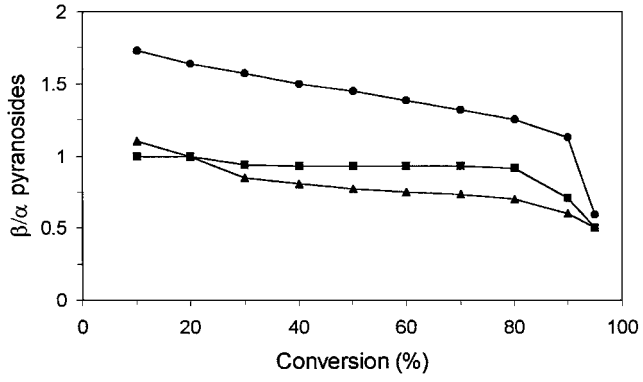

FIG. 9. Plot of the β/α ratio of butyl-D-glucopyranosides versus D-glucose conversion in the presence of different catalysts (●, HY15; ❍, PTSA; ▲, HBEA12.5) for glycosylation of glucose (4.8 g) with *n*-butanol (50 ml) at 383 K and 1000 rpm of agitation speed.

We have first determined the most stable conformations of the different glucosides by conformational analysis. The following stability order, from the more to the less stable, is obtained: α-pyranose>β-pyranose>β-furanose>α-furanose (Table 6), six-membered rings (pyranosides) being more stable than five-membered rings (furanosides) (31). Although the molecules are considered under vacuum at 0 K for conformational analysis calculations, the computed energy orders for free sugars are in good agreement with the experimental results. The α-pyranose form is more stable because of the endoanomeric effect (32) and, on the contrary, the α-furanose form is less stable because of *cis* interactions between the alkoxy group on C_1 and the hydroxyl group on C_2 (20). The satisfactory results obtained for molecular modeling of free sugars prompted us to investigate further the butyl-D-glucoside forms. Once again, calculations agree quite well with the literature data. The same stability order is obtained (Table 6), and the differences in calculated energies for the different anomers are conventional ones (33).

Second, from the most stable conformations determined for glycosides, it was then possible to estimate the size of the different conformers from projections in different plans. The corresponding ring diameter in which the conformers can enter was assessed as the critical diameter (Table 6). As expected for five-membered rings compared to six-membered rings, the critical diameters of furanosides are less important than those of pyranosides. It clearly appears from these calculations that butyl-D-glucopyranosides have a critical diameter close to that of D-glucose and that there is no significant difference between α- and β-pyranosides. With a mean value of 6.3 Å for the critical diameter of both conformers, the stereoselectivity of the glycosylation

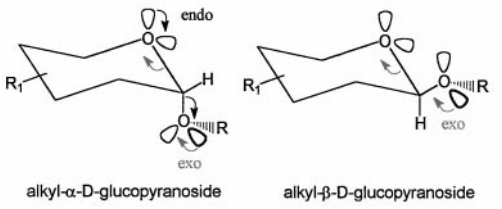

FIG. 10. Illustration of endo- and exoanomeric effects (R1, hydroxyl groups).

reaction over H–Y zeolites cannot result from products shape selective properties only. Indeed, transition states selective properties cannot be ruled out if we consider the influence of stereoelectronic effects.

Let us now focus our attention on the different anomeric effects which take place in alkyl-D-glucopyranosides (Fig. 10). An endoanomeric effect takes place if an electron lone pair on the endocyclic oxygen is antiperiplanar to the exocyclic C–O bond. In this manner, a stabilizing interaction exists between this electron lone pair and the antibonding σ^* orbital of the C–O anomeric bond (34). Such a stabilization, only occurring with the α-pyranoside form, leads to a decrease in free energy of about 0.5 kcal mol^{-1} as already calculated with AmberS by Still *et al.* (33). It is also worth mentioning the existence of an exoanomeric effect based on the same delocalization between the electron lone pair of the exocyclic oxygen and the antibonding σ^* orbital of the endocyclic C–O bond (35).

(c) Stereoelectronic effects. Stereoelectronic effects are a key element in order to understand the chemical reactivity of organic reactions (36). It is generally accepted now that stereoelectronic effects play an important role in glycoside hydrolytic processes (37).

For homogeneous acid-catalyzed hydrolysis of alkyl-D-glucopyranosides, it has already been shown that the β-anomer hydrolyzes 2 or 3 times faster than the α-anomer (38). In order to understand why the β-anomer, which does not present the required electron lone pair orientation to hydrolyze with stereoelectronic assistance due to endo-anomeric effect, hydrolyzes faster than the α-anomer; the formation of a twist-boat transition state must be considered and then the occurence of reverse anomeric effect (Fig. 11).

The reverse anomeric effect is a stabilizing electronic effect taking place in charged species and leading to preferred conformations which have the positively charged anomeric substituent in the equatorial position as it occured with the pyridinium group (39). When the positively charged atom is gauche to the two electron lone pairs, a maximum stabilizing effect, like in the β-anomer, is obtained. As it was rationalized by Deslongchamps (37) in the case of protonated alkoxy groups in hydrolysis of alkylglucopyranosides (Fig. 11), it results that, after protonation of the OR group

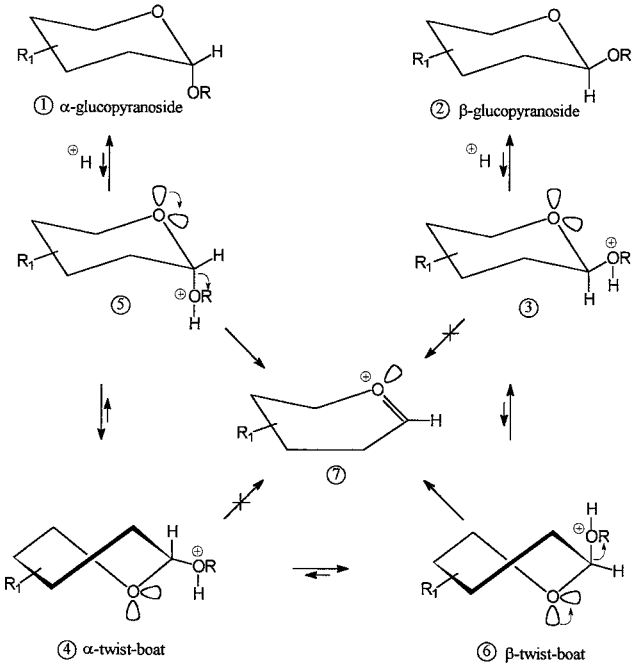

FIG. 11. Reaction pathway for hydrolysis of alkyl-D-glucopyranosides taking into account the relative stabilities from the more stable (1) to the less stable (7) intermediate.

of the β-anomer ② to give the intermediate ③ the reverse anomeric effect occurs when the leaving group is gauche to the two electron lone pairs of the endocyclic oxygen atom. Then it would have to undergo a conformational change to the β-twist-boat form ⑥ for stereoelectronic assistance to the cleavage of the leaving group. For the α-anomer ①, the stereoelectronic assistance can directly occur from the intermediate ⑤ but it will undergo a conformational change to the more stable α-twist-boat form ④ because of the reverse anomeric effect. Both anomers must therefore form the same half-chair intermediate ⑦ to hydrolyze. The result of the competitive formation of the two possible intermediates ④ and ⑦ to hydrolyze with stereoelectronic assistance in the α-anomer ⑤ then leads to a hydrolysis rate lower for the α-anomer than for the β-anomer.

Such an assumption also took into account the reactivity of conformationally rigid bicyclic acetals (Fig. 12) for which the α-anomer hydrolyzes 1.5 times faster than the β-anomer (40). The formation of a twist-boat form is no longer favored because of the rigidity of the bicyclic system. Consequently, the α-anomer, which has the required orientation for

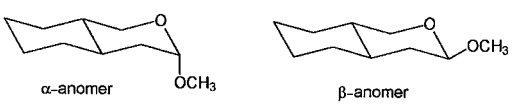

FIG. 12. Bicyclic acetals used as hydrolysis models in homogeneous catalysis.

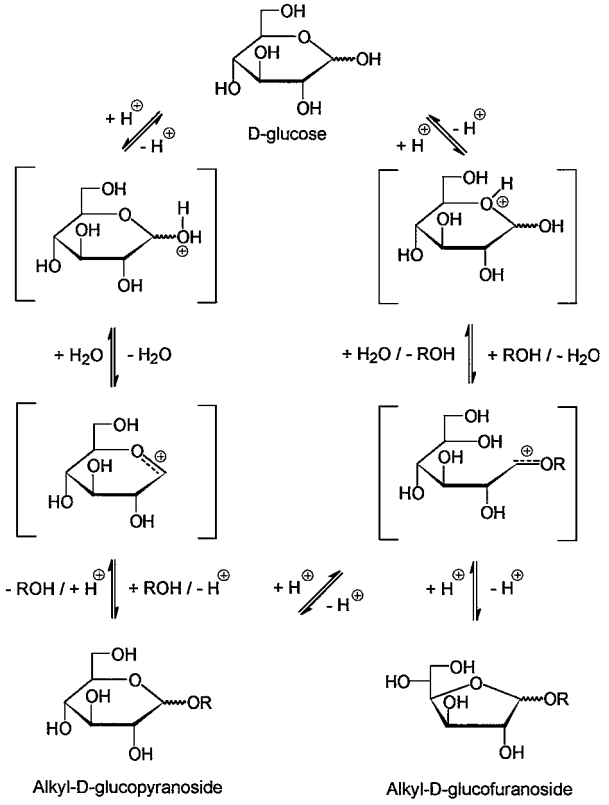

SCHEME 2. Glycosylation pathway involving microreversibility principle.

stereoelectronic assistance after protonation, hydrolyzes faster than the β-anomer which cannot adopt a twist-boat conformation favoring stereoelectronic assistance.

For hydrolysis of methyl α- and β-D-glucopyranosides in the presence of protonic zeolites, a similar behavior is found (41). In the absence of steric constraints, stereoelectronic effects will apply. Moreover, an additional effect resulting from the presence of an electron deficient surface is observed. The favorable orientation of the electron lone pair(s) leads to both easier protonation and adsorption of oxygen atoms. In that way, methyl β-D-glucopyranoside was found to hydrolyze faster than methyl β-D-glucopyranoside by a factor of around 6 in the presence of a HY zeolite with a Si/Al ratio of 15 (41). However, if the internal pore diameter is reduced as in H-form mordenites, the formation of twist-boat forms is more difficult and the β/α ratio is equal to 1 (42).

When the methyl substituent is replaced by a bulkier one such as a glucose moiety as in disaccharides, maltose (α-1-4 linkage), and cellobiose (β-1-4 linkage), it was shown that maltose (α-anomer) hydrolyzed 3 times faster than cellobiose (β-anomer) in the presence of the HY15 zeolite (43). The rigidity of the disaccharide system is then reinforced because of the presence of microporous cavities, and then the α-linked anomer will hydrolyze faster since twist-boat formation is no longer favored because of steric hindrance within the intracrystalline network.

By virtue of the microreversibility principle, the same transition states should be invoked for the formation of alkyl-D-glucopyranosides and hydrolysis thereof, with the formation of a cyclic carboxonium ion intermediate (Scheme 2). In this manner, it is possible to explain why the HY zeolite favors the β selectivity, whereas the HBEA zeolite will favor the α one. Within the large pores of HY zeolite (cavities with a diameter of 11.8 Å), the formation of twist-boat forms can occur and the β-anomer will be preferentially formed via the ⑦ → ⑥ → ③ → ② route (Fig. 11). In the more confined HBEA zeolite with only 7.6×6.4 Å channels, the formation of twist-forms will be no longer favored, and the ⑦ → ⑤ → ① route (Fig. 11) leading to the more stable α-anomer will be preferred. It should be noted that the anomeric β/α ratio will drop to its thermodynamical value at a nearly complete conversion of glucose.

CONCLUSION

Several conclusions can be drawn from this work: (i) the direct synthesis of butyl-D-glucosides starting from glucose and *n*-butanol is easily achieved in the presence of acid dealuminated Y-faujasites as catalysts, (ii) the amount of oligomers is significantly reduced compared to the homogeneous catalyzed reaction, (iii) the selectivity to the β-anomer is higher for H–Y compared to H–BEA zeolite, (iv) the kinetic reaction scheme proposed, involving both consecutive and competitive steps, accounts for the higher β/α observed with Y-faujasites as due to the result of stereoelectronic effects associated with the shape selective properties of the catalysts in the transition states, (v) the factors of reactivity invoked in the direct glycosylation reaction are of the same nature as those involved in the reverse reaction, i.e., hydrolysis of alkyl-D-glucopyranosides, thus allowing for the first time the consideration of the principle of microreversibility for reactions catalyzed by solids, and, finally, (vi) such a process could be easily transposed to the synthesis of long chain alkyl-D-glucosides.

REFERENCES

1. Hensen, H., Busch, P., Krächter, H. U., and Tesmann, H., *Tensid. Surf. Det.* **30**, 116 (1993).
2. Mentech, J., Beck, R., and Burzio, F., *in* "Carbohydrates as Raw Organic Materials" (G. Descotes, Ed.), p. 185. VCH, Weinheim, 1993.
3. Hughes, F. A., and Lew, B. W., *J. Am. Oil Chem. Soc.* **47**, 162 (1970).
4. Jeffrey, G. A., *Acc. Chem. Res.* **19**, 168 (1986).
5. Fischer, E., *Ber. Deutsch. Chem. Ges.* **26**, 2400 (1893).
6. Groen, J., WO 95/07915 (1995).
7. Van Bekkum, H., De Goede, A. T. J. W., Van Der Leij, I. G., Van Der Heijden, A. M., and Van Rantwijk, F., WO 96/36640 (1996).
8. Biermann, M., Schmid, K., and Schulz, P., *Starch/Stärke* **45**, 281 (1993).

9. Straathof, A. J. J., Romein, J., Van Rantwijk, F., Kieboom, A. P. G., and Van Bekkum, H., *Starch/Stärke* **39**, 362 (1987).
10. Straathof, A. J. J., Van Bekkum, H., and Kieboom, A. P. G., *Starch/Stärke* **40**, 229 (1988).
11. Brochette, S., Descotes, G., Bouchu, A., Queneau, Y., Monnier, N., and Petrier, C., *J. Mol. Catal. A Chemical* **123**, 123 (1997).
12. Corma, A., Iborra, S., Miquel, S., and Primo, J., *J. Catal.* **161**, 713 (1996).
13. Matsumura, S., Imai, K., Yoshikawa, S., Kawada, K., and Uchibori, T., *J. Am. Oil Chem. Soc.* **67**, 996 (1990).
14. Goodby, J. W., Haley, J. A., Mackenzie, G., Watson, J., Plusquellec, D., and Ferrieres, V., *J. Mater. Chem.* **5**, 2209 (1995).
15. Chapat, J.-F., and Moreau, C., *Carbohydr. Lett.* **3**, 25 (1998).
16. (a) Joffre, J., Geneste, P., Guida, A., Szabo, G., and Moreau, C., *Stud. Phys. Theor. Chem.* **71**, 409 (1989); (b) Joffre, J., and Joffre F., AnaCin, Langage et informatique, Toulouse (1995).
17. Bond, G. C., "Heterogeneous Catalysis: Principle and Applications," Oxford Chemistry Series No. 34 (P. W. Atkins, J. S. E. Holker, and A. K. Holliday, Eds.), 2nd Ed., Clarendon Press, Oxford, 1987.
18. Weisz, P., *Chem. Eng. Prog.* **55**, 29 (1957).
19. Capon, B., *Chem. Rev.* **69**, 440 (1969).
20. Collins, P., and Ferrier, R., "Monosaccharides." Wiley, Chichester, 1995.
21. Levene, P. A., Raymond, A. L., and Dillon, R. T., *J. Biol. Chem.* **95**, 699 (1932).
22. Shafizadeh, F., *Adv. Carbohydr. Chem.* **13**, 9 (1958).
23. Lecomte, J., Finiels, A., Geneste, P., and Moreau, C., *J. Mol. Catal. A Chemical* **133**, 283 (1998).
24. Barthomeuf, D., *Mater. Chem. Phys.* **17**, 49 (1987).
25. Richard, F., Carreyre, H., and Pérot, F., *J. Mol. Catal. A Chemical* **103**, 51 (1995).
26. Camblor, M. A., Corma, A., Iborra, S., Miquel, S., Primo, J., and Valencia, S., *J. Catal.* **172**, 76 (1997).
27. Smirnyagin, V., and Bishop, C. T., *Can. J. Chem.* **46**, 3085 (1968).
28. Mowery, D. F., *J. Am. Chem. Soc.* **77**, 1667 (1955).
29. Meier, W. M., Olson, D. H., and Baerlocher, Ch., "Atlas of Zeolite Structure Types," 4th revised version. Butterworth-Heinemann, London,1996.
30. Homans, S. W., *Biochem.* **29**, 9110 (1990).
31. Angyal, S. J., *Adv. Carbohydr. Chem. Biochem.* **42**, 15 (1984).
32. Senderowitz, H., Parish, C., and Clark Still, W., *J. Am. Chem. Soc.* **118**, 2078 (1996).
33. Senderowitz, H., and Clark Still, W., *J. Org. Chem.* **62**, 1427 (1997).
34. Lemieux, R. U., and Chü, N. J., *Abstr. Pap. Am. Chem. Soc.* **133**, 31N (1958).
35. Lemieux, R. U., Pavia, A. A., Martin, J. C., and Watanabe, K. A., *Can. J. Chem.* **47**, 4427 (1969).
36. Deslongchamps, P., "Stereoelectronic Effects in Organic Chemistry" (J. E. Baldwin, Ed.), Organic Chemistry Series, Vol. I. Pergamon Press, Oxford, 1983.
37. Deslongchamps, P., *Pure App. Chem.* **65**, 1161 (1993).
38. Be Miller, J. N., and Doyle, E. R., *Carbohydr. Res.* **20**, 23 (1971).
39. Lemieux, R. U., and Morgan, A. R., *Can. J. Chem.* **43**, 2205 (1965).
40. Van Eickeren, P., *J. Org. Chem.* **45**, 4641 (1980).
41. Le Strat, V., and Moreau, C., *Catal. Lett.* **51**, 219 (1998).
42. Le Strat, V., and Moreau, C., unpublished results.
43. Moreau, C., Durand, R., Duhamet, J., and Rivalier, P., *J. Carbohydr. Chem.* **16**, 709 (1997).